Electronic Supplementary Material (ESI) for Analytical Methods.
This journal is © The Royal Society of Chemistry 2022

Electronic Supplementary Information

Highly Selective and Discriminative Detection of Small Alcohols Based on a Dual-emission Macrocyclic Samarium Complex

Chengjian Zhang, Sichen Li, Ruijie Zheng, Shengdi Tai, Kang Yang, Kun Zhang*
Department of Chemistry, Key Laboratory of Surface & Interface Science of Polymer Materials of Zhejiang Province, Zhejiang Sci-Tech University, Hangzhou 310018, China

Crystal structure determination and refinement

The single-crystal sample of complex **Sm-2$_r$** was covered with glue and mounted on glass fiber for data collection. Crystallographic data were collected at 150(2) K on a Bruker SMART 1K CCD diffractometer, using graphite mono-chromated MoKα radiation (λ = 0.71073 Å). Absorption corrections were performed to all data and the structure was solved by direct method and refined by full-matrix least-squares method on F_{obs}^2 by using the SHELXTL-PC software package [1]. All non-H atoms were anisotropically refined and all hydrogen atoms were inserted in the calculated positions assigned fixed isotropic thermal parameters and allowed to ride on their respective parent atoms. A summary of the crystal data, experimental details and refinement results for **Sm-2$_r$** was listed in Table S1. Selected bond lengths and bond angles of **Sm-2$_r$** were tabulated in Table S2, and hydrogen-bonding parameters were shown in Table S3.

References

[1] G. M. Sheldrick, SHELXTL (Version 6.10). Software Reference Manual; Madison, Wisconsin (USA): Bruker AXS, Inc.: 2000.

Tables

Table S1. Crystal data and structural refinements for complex **Sm-2$_r$**.

Complex	**Sm-2$_r$**
Empirical formula	$C_{33}H_{38}C_{12}N_5O_{10}Sm$, 2($CH_3CN$)
Formula weight	968.04
Temperature / K	150(2)
Wavelength / Å	0.71073
Crystal Size (mm)	0.15×0.17×0.23
Crystal system	Monoclinic
Space group	$P2_1/n$
a / Å	16.914(1)
b / Å	14.088(1)
c / Å	17.176(1)
α / °	90
β / °	99.958(2)
γ / °	90
V / Å^3	4031.0(6)
Z / D_{calcd} (g / cm^3)	4 / 1.595
F(000)	1964
μ / mm^{-1}	1.654
h_{min} / h_{max}	–20 /20
k_{min} / k_{max}	–17 / 17
l_{min} / l_{max}	–21 / 21
Data / parameters	7944 / 519
R_1, wR_2 [$I > 2\sigma(I)$]^a	R_1 = 0.0358, wR_2 = 0.0673
R_1, wR_2 (all data)^a	R_1 = 0.0605, wR_2 = 0.0760
S	1.05
Max/min $\Delta\rho$/e Å^{-3}	1.75 / –0.73

^{a} $R_1 = \Sigma||Fo|-|Fc|| / \Sigma|Fo|$, $wR_2 = [\Sigma[w(Fo^2-Fc^2)^2] / \Sigma w(Fo^2)^2]^{1/2}$

Table S2. Selected bond distances (Å) and angles (°) in complex **Sm-2$_r$**.

Bond distances		Bond angles	
Sm-2$_r$			
Sm1–O1	2.358(3)	O1–Sm1–O2	116.0(1)
Sm1–O2	2.707(3)	O1–Sm1–O3	141.6(1)

Sm1–O3	2.695(3)	O1–Sm1–O4	67.3(1)
Sm1–O4	2.304(3)	O1–Sm1–O5	135.7(1)
Sm1–O5	2.533(3)	O1–Sm1–O6	92.9(1)
Sm1–O6	2.564(3)	O1–Sm1–O8	74.2(1)
Sm1–O8	2.570(3)	O1–Sm1–O9	82.9(1)
Sm1–O9	2.512(3)	O1–Sm1–N2	68.8(1)
Sm1–N2	2.633(3)	O1–Sm1–N3	132.8(1)
Sm1–N3	2.718(3)	O2–Sm1–O3	58.7(1)
		O2–Sm1–O4	176.4(1)
		O2–Sm1–O5	66.3(1)
		O2–Sm1–O6	108.2(1)
		O2–Sm1–O8	67.6(1)
		O2–Sm1–O9	107.0(1)
		O2–Sm1–N2	61.8(1)
		O2–Sm1–N3	111.0(1)
		O3–Sm1–O4	118.0(1)
		O3–Sm1–O5	80.1(1)
		O3–Sm1–O6	125.5(1)
		O3–Sm1–O8	69.0(1)
		O3–Sm1–O9	65.5(1)
		O3–Sm1–N2	120.5(1)
		O3–Sm1–N3	63.7(1)
		O4–Sm1–O5	112.5(1)
		O4–Sm1–O6	72.5(1)
		O4–Sm1–O8	113.0(1)
		O4–Sm1–O9	72.7(1)
		O4–Sm1–N2	121.5(1)
		O4–Sm1–N3	65.6(1)
		O5–Sm1–O6	50.2(1)
		O5–Sm1–O8	133.1(1)
		O5–Sm1–O9	141.0(1)
		O5–Sm1–N2	76.3(1)
		O5–Sm1–N3	69.6(1)
		O6–Sm1–O8	161.5(1)
		O6–Sm1–O9	142.7(1)
		O6–Sm1–N2	73.1(1)
		O6–Sm1–N3	77.4(1)

O8–Sm1–O9	50.4(1)
O8–Sm1–N2	89.7 (1)
O8–Sm1–N3	121.1(1)
O9–Sm1–N2	136.7(1)
O9–Sm1–N3	78.7(1)
N2–Sm1–N3	144.4(1)

Table S3. Intramolecular hydrogen bonding parameters (Å, °) in complex **Sm-2$_r$**.

D–H···A	D–H	H···A	D···A	∠DHA
Sm-2$_r$				
N1–H1···O1	1.00	2.19	2.884(4)	125
N1–H1···O4	1.00	1.84	2.626(4)	133

Table S4. Bond distances ($d_{Sm,j}$), bond valences ($v_{Sm,j}$) and total samarium atom valence (V_{Sm}) in the crystal structure of complex **Sm-2$_r$**.

Compound	Atom	Donor type	$d_{Sm,j}$/Å	$v_{Sm,j}$	V_{Sm}
Sm-2$_r$	O1	HL2$_r^-$	2.358	0.491	3.162
	O2	HL2$_r^-$	2.707	0.191	
	O3	HL2$_r^-$	2.695	0.198	
	O4	HL2$_r^-$	2.304	0.568	
	O5	NO_3^-	2.533	0.306	
	O6	NO_3^-	2.564	0.282	
	O8	NO_3^-	2.570	0.277	
	O9	NO_3^-	2.512	0.324	
	N2	HL2$_r^-$	2.633	0.292	
	N3	HL2$_r^-$	2.718	0.232	

Table S5. Parameters of polarity, viscosity and dielectric constant of alcohol solvents

Solvent	Viscosity (cp 25 ℃)	Polarity	Dielectric constant (F/m 50 ℃)
Methanol	0.54	6.60	27.80
ethanol	1.08	4.30	20.78
i-propanol	2.04	4.30	20.2
n-propanol	1.95	4.00	20.3(25 ℃)
n-butanol	2.57	3.70	14.31

Isobutyl alcohol	3.40	3.00	/
n-pentanol	3.51	/	15.56(25 ℃)
n-Hexanol	4.59	/	13.25(25 ℃)
n-heptanol	5.94	/	11.79(25 ℃)
cyclopropanol	/	/	/
cyclobutanol	/	/	/
cyclopentanol	/	/	/
cyclohexanol	4.6	/	/
cycloheptanol	/	/	/
Ethylene glycol	16.95	6.90	38.66(23 ℃)
1,3-propanediol	56.00	/	/
1,2-propanediol	40.40	/	/
Glycerol	934	/	42.5(23 ℃)

Figures

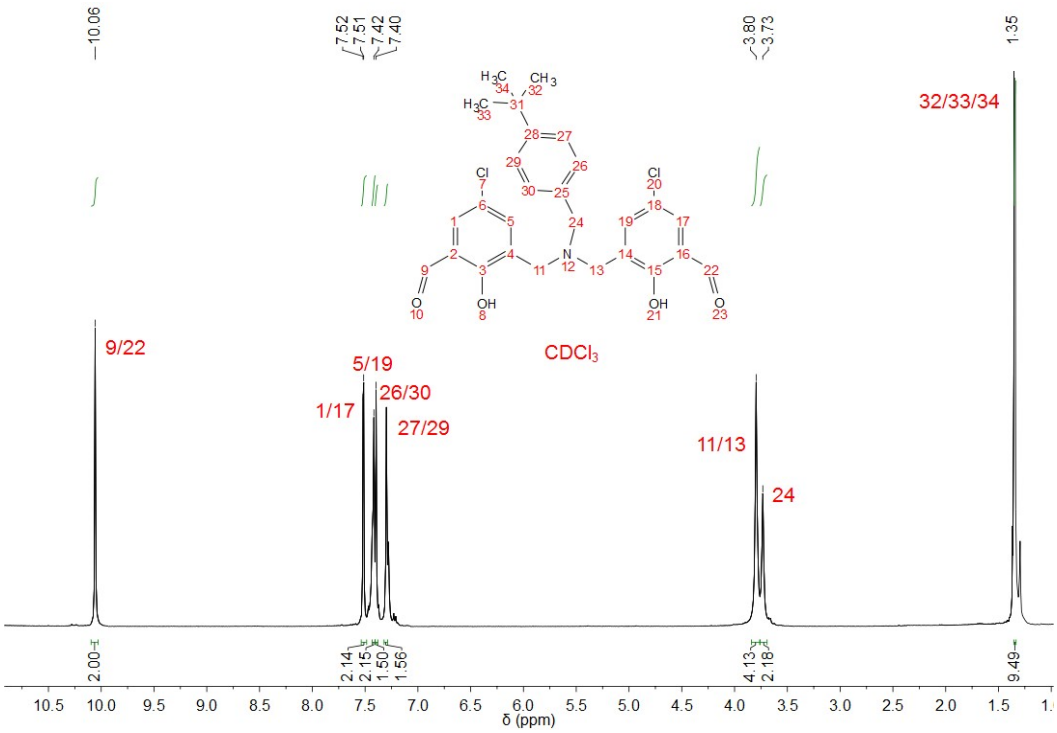

Fig. S1. ^{1}H NMR spectrum of dialdehyde H_2Q_r in $CDCl_3$.

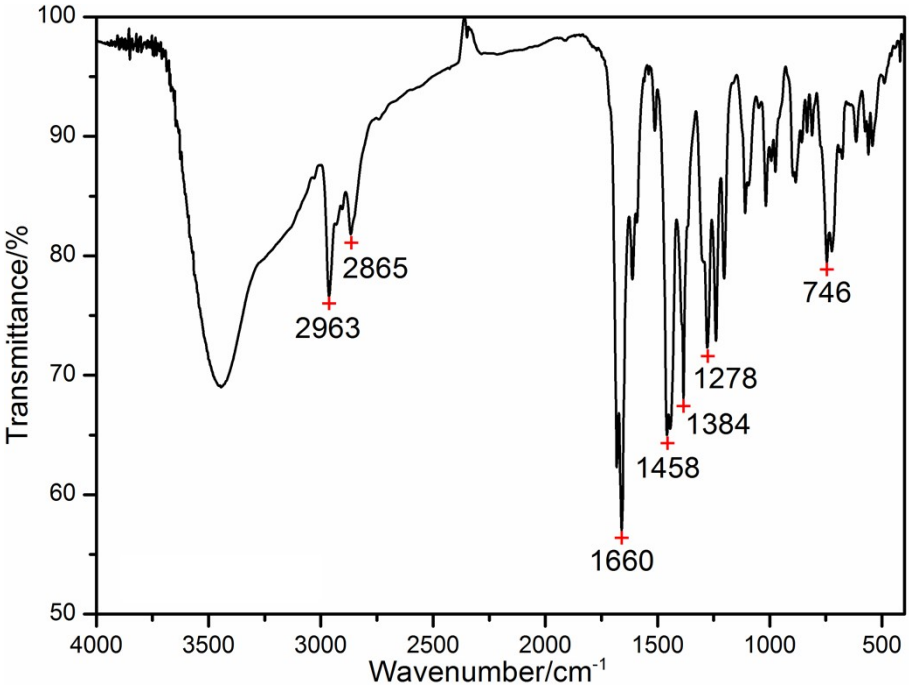

Fig. S2. FT-IR spectrum of dialdehyde H_2Q_r.

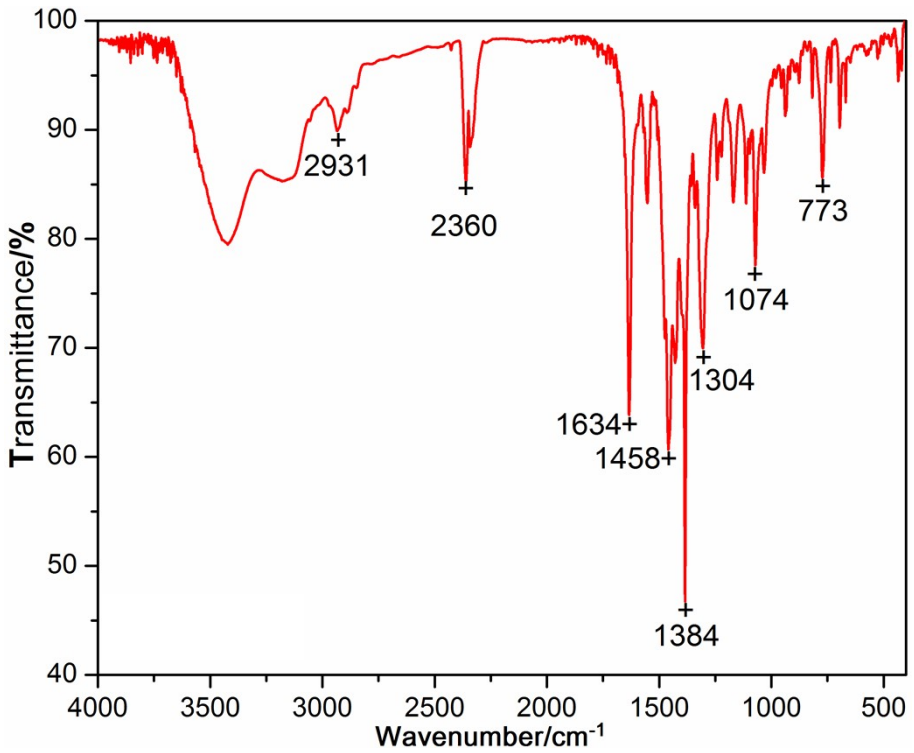

Fig. S3. FT-IR spectrum of macrocyclic Sm(III) complex **Sm-2$_r$**.

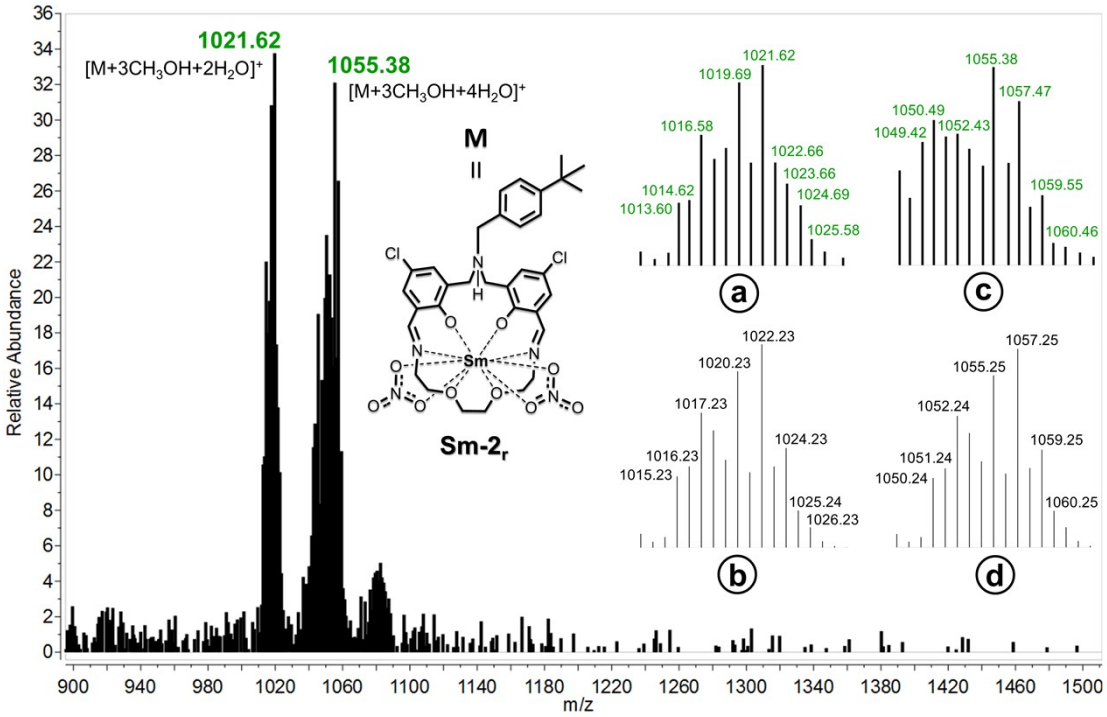

Fig. S4. ESI-MS (positive) of [1+1] Schiff-base macrocyclic mononuclear Sm(III) complex **Sm-2$_r$** together with the inserted experimental (**a** and **c**) and simulative (**b** and **d**, calculation for [$C_{36}H_{54}Cl_2N_5O_{15}Sm$] and [$C_{36}H_{58}Cl_2N_5O_{17}Sm$], respectively) peaks of isotopic distribution corresponding to the peaks at m/z = 1021.62 and 1055.38.

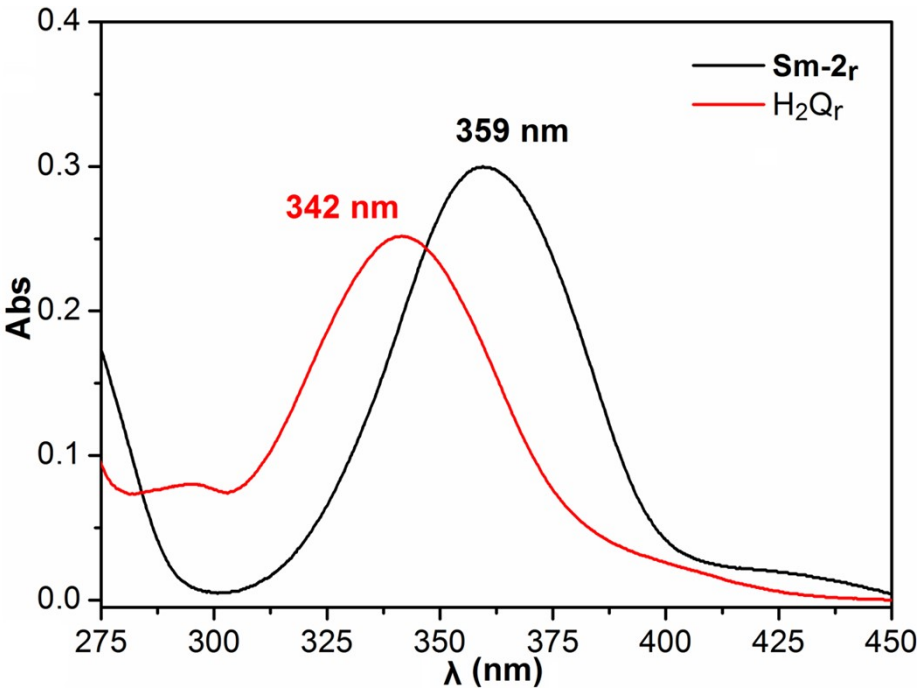

Fig. S5. UV-vis absorption spectra of H_2Q_r (25 μM) and **Sm-2$_r$** (25 μM) in CH_3OH.

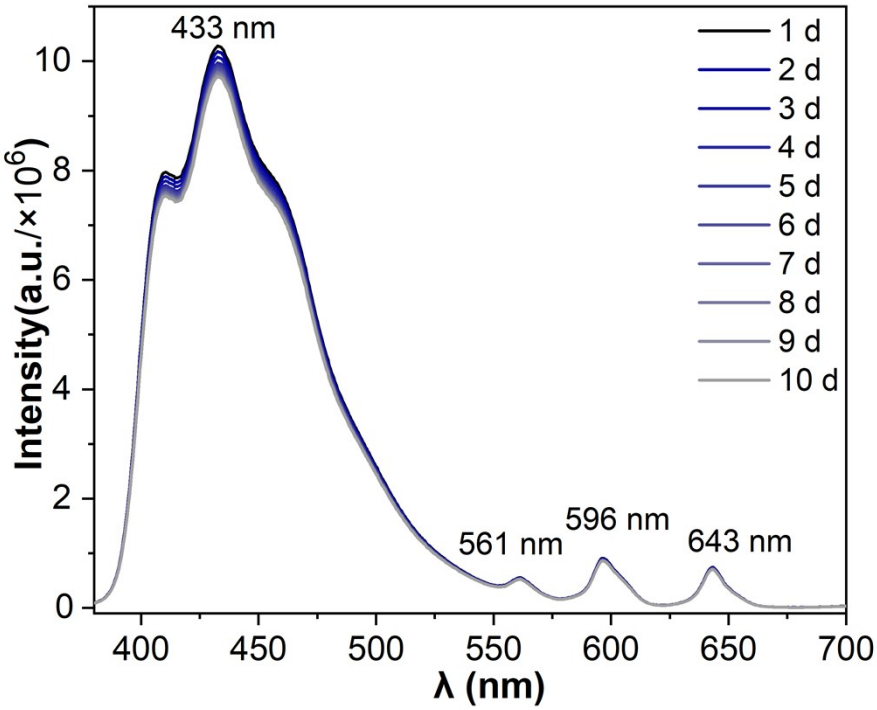

Fig. S6. Time-dependent emission spectra (λ_{ex} = 359 nm) of complex **Sm-2$_r$** (25 μM) in CH_3OH.

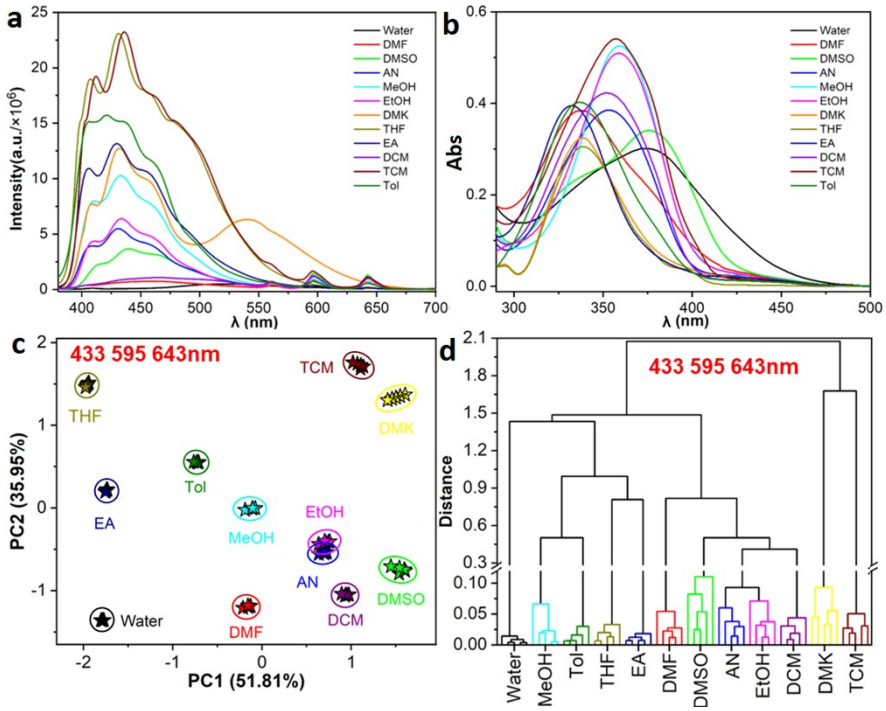

Fig. S7. Fluorescence (a) UV-vis absorption (b) spectra of **Sm-2$_r$** (50 μM) mixed with different solvents. PCA (c) and HCA (d) plots derived from fluorescence responses of the **Sm-2$_r$** (50 μM) toward twelve solvents upon three fluorescence channels (433, 596 and 643 nm).

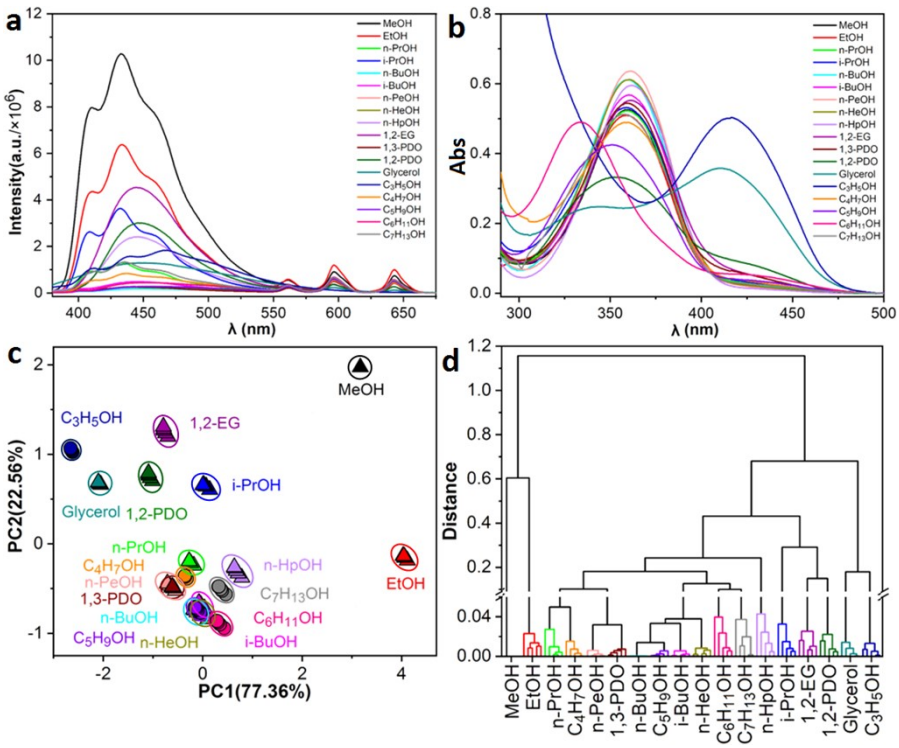

Fig. S8. Fluorescence (a) UV-vis absorption (b) spectra of **Sm-2$_r$** (50 μM) mixed with different alcohols. PCA (c) and HCA (d) plots for fluorescence responses of **Sm-2$_r$** (50 μM) toward eighteen alcohols upon three fluorescence channels (433, 596 and 643 nm).

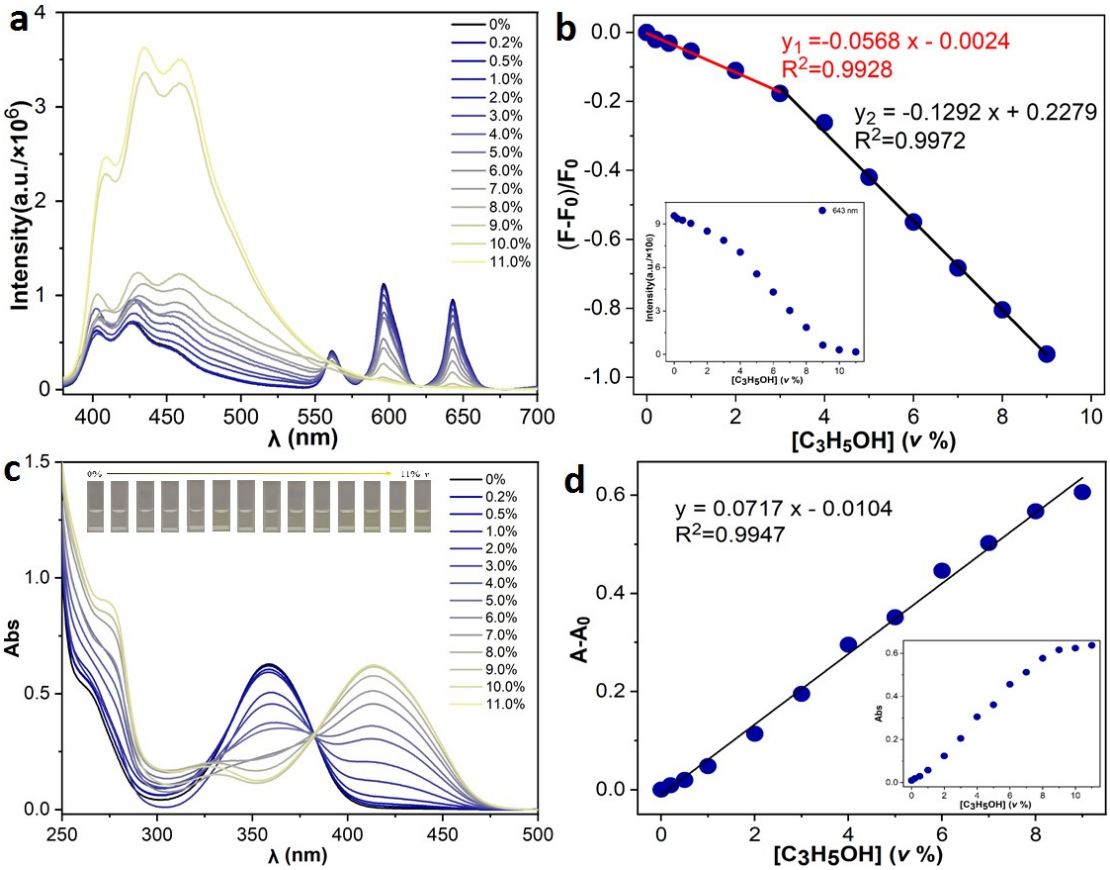

Fig. S9. (a) Fluorescence plot of **Sm-2$_r$** (50 μM) toward C_3H_5OH with different concentration. (0-3%, 3-10% *v/v*). (b) concentration function diagram of 643 nm emission band pair C_3H_5OH based on **Sm-2$_r$** (50 μM). (c) absorption changes of **Sm-2$_r$** (50 μM) upon increasing contents of C_3H_5OH. (d) linearity of absorbance (413 nm) versus the concentration of C_3H_5OH.

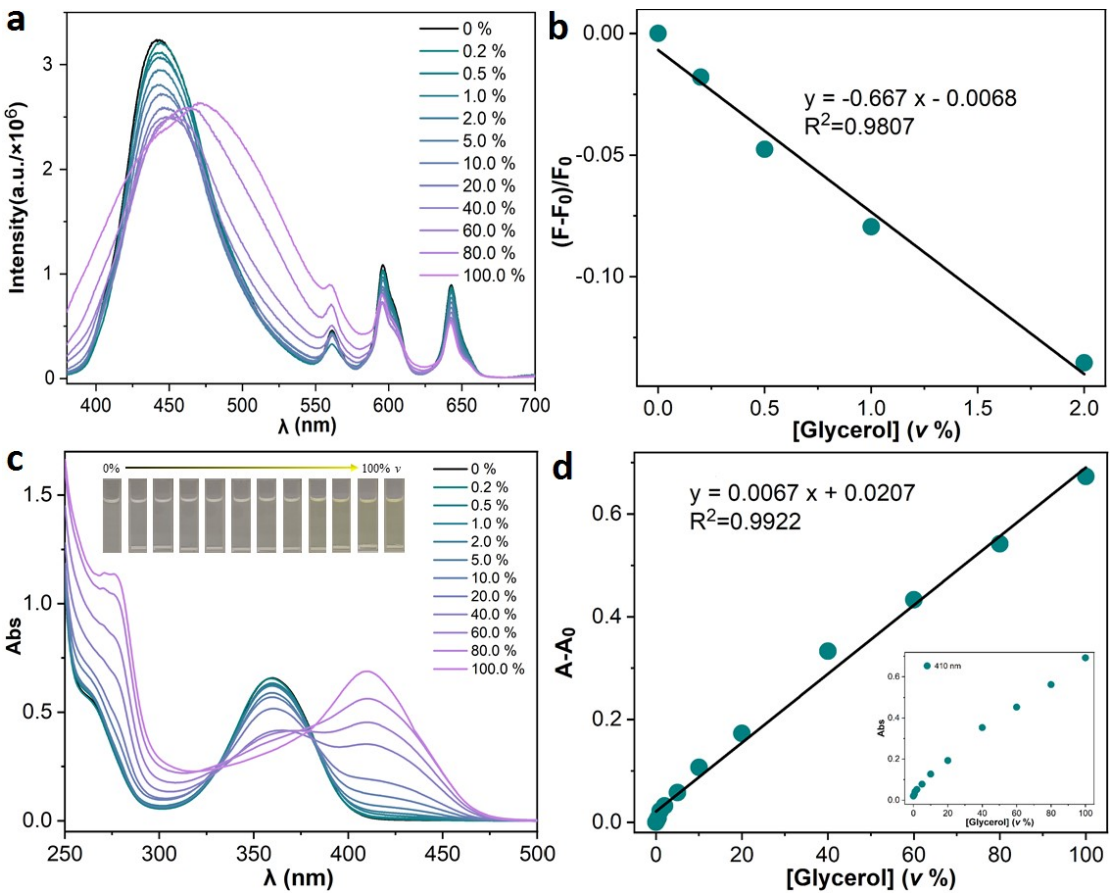

Fig. S10. (a) Fluorescence plot of **Sm-2$_r$** toward glycerol with different concentration. (b) concentration function diagram of 643 nm emission band pair glycerol based on **Sm-2$_r$** (50μM). (c) absorption changes of **Sm-2$_r$** (50 μM) upon increasing contents of glycerol. (d) Linearity of absorbance (413 nm) versus the concentration of glycerol.

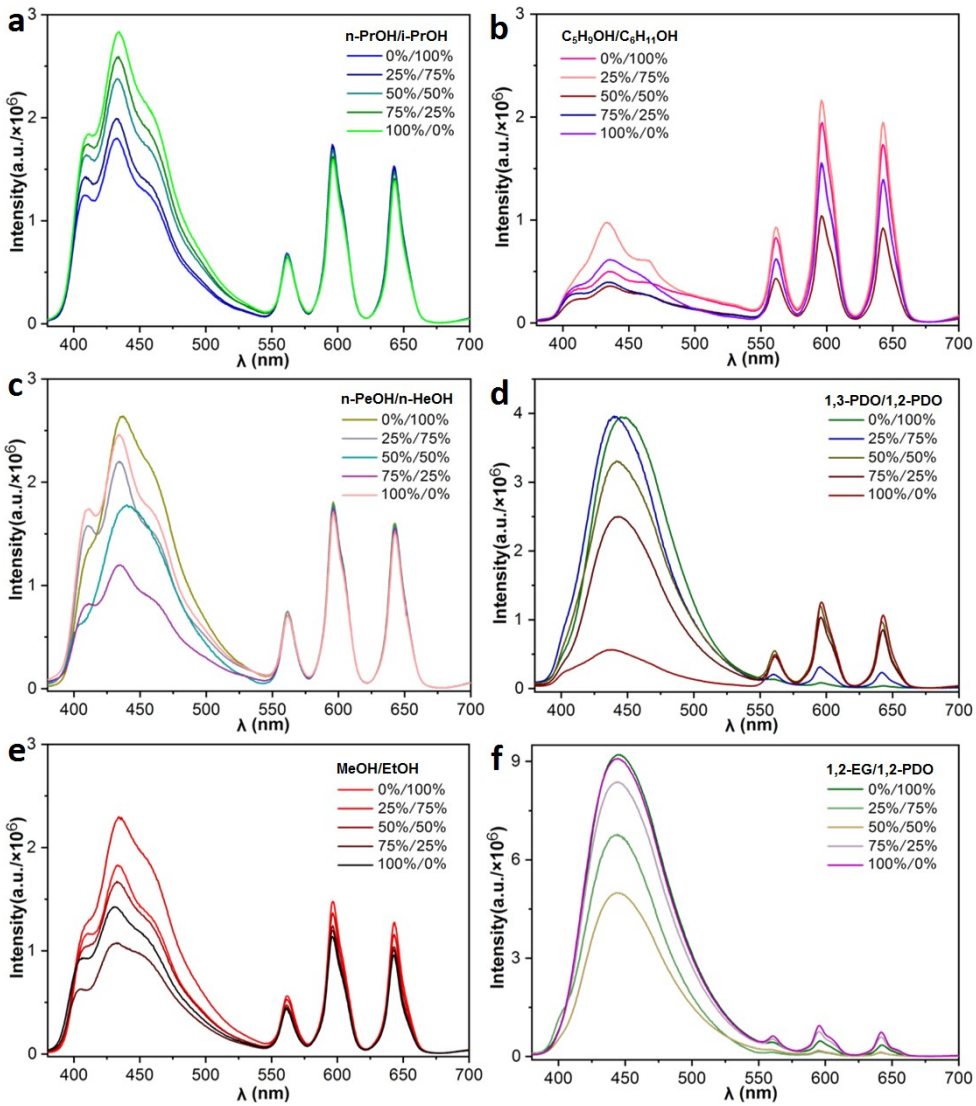

Fig. S11. Fluorescence spectra originate from respond of Sm-2r sensor toward mixtures (a) n-PrOH/i-PrOH (b) $C_5H_9OH/C_6H_{11}OH$ (c) n-PeOH/n-HeOH (d) 1,3-PDO/1,2-PDO (e) MeOH/EtOH and (f) 1,2-EG/1,2-PDO at different volume ratio (*v*%/*v*%, i.e., 0%/100%, 25%/75%, 50%/50%, 75%/25% and 100%/0%).

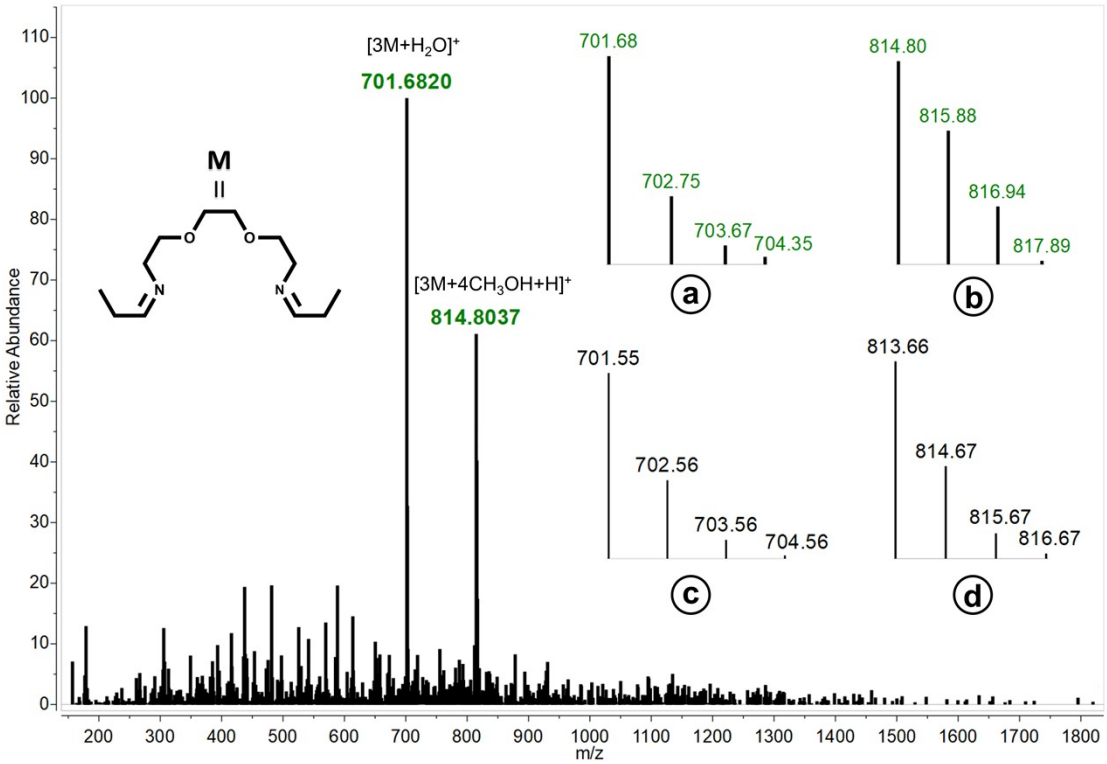

Fig. S12. ESI-MS (positive) of Sm(III)-macrocycle **Sm-2$_r$** (50.0 μM) mixed with C_3H_5OH (4 mL) together with its inserted experimental (a and b) and simulative (c and d) calculation for [$C_{36}H_{74}N_6O_7$] and [$C_{40}H_{89}N_6O_{10}$] respectively peaks of isotopic distribution corresponding to the peaks at m/z = 701.6820 and 814.8037.

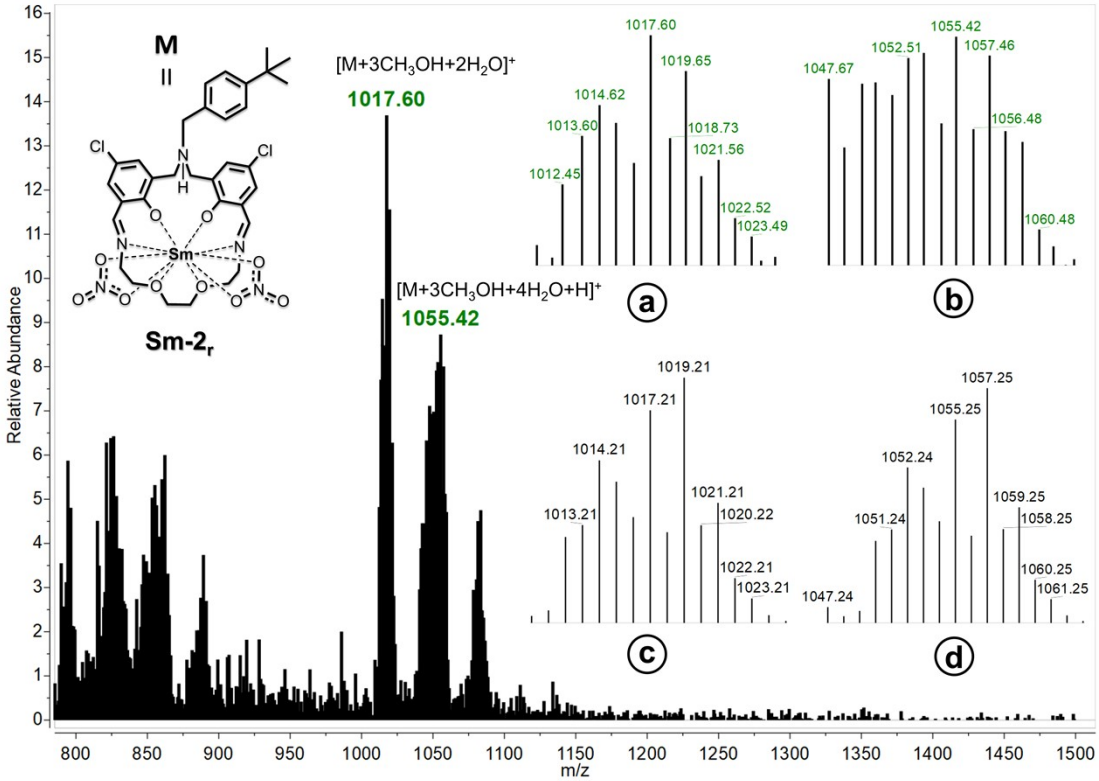

Fig. S13. ESI-MS (positive) of Sm(III)-macrocycle **Sm-2$_r$** (50.0 μM) mixed with

glycerol (4 mL) together with its inserted experimental (**a** and **b**) and simulative (**c** and **d**), calculation for [$C_{36}H_{54}Cl_2N_5O_{15}Sm$] and [$C_{36}H_{59}Cl_2N_5O_{17}Sm$], respectively peaks of isotopic distribution corresponding to the peaks at m/z = 1017.60 and 1055.42.